AD-A191 326 UNIVERSAL DETECTION OF IONS BY REPLACEMENT-ION CHROMATOGRAPHY EMPLOYING A.. (U) INDIANA UNIV AT BLOOMINGTON DEPT OF CHEMISTRY L J GALANTE ET AL. 1/1

UNCLASSIFIED 22 FEB 88 INDU/DC/GMH/TR-88-21 F/G 7/4 NL

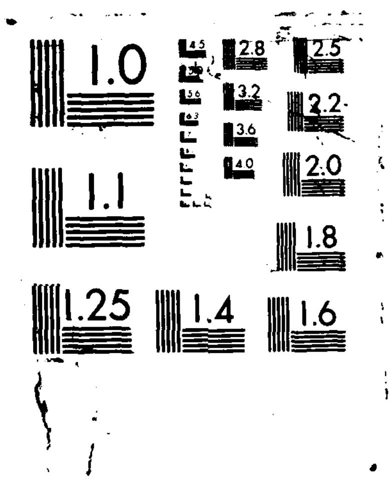
1.0
2.8
2.5
3.2
2.2
3.6
4.0
2.0
1.1
1.8
1.25
1.4
1.6

UNCLASSIFIED **DTIC FILE COPY** (2)

SECURITY CLASSIFICATION OF THIS PAGE

REPORT DOCUMENTATION PAGE

AD-A191 326

1b. RESTRICTIVE MARKINGS: NA	
2b. DECLASSIFICATION / DOWNGRADING SCHEDULE: NA	3. DISTRIBUTION / AVAILABILITY OF REPORT: Distribution Unlimited; Approved for Public Release
4. PERFORMING ORGANIZATION REPORT NUMBER(S): INDU/DC/GMH/TR-21	5. MONITORING ORGANIZATION REPORT NUMBER(S): NA
6a. NAME OF PERFORMING ORGANIZATION: Indiana University; 6b. OFFICE SYMBOL (If applicable): NA	7a. NAME OF MONITORING ORGANIZATION: ONR
6c. ADDRESS (City, State, and ZIP Code): Department of Chemistry, Bloomington, IN 47405	7b. ADDRESS (City, State, and ZIP Code): 800 N. Quincy Street, Arlington, VA 22217
8a. NAME OF FUNDING / SPONSORING ORGANIZATION; 8b. OFFICE SYMBOL (If applicable)	9. PROCUREMENT INSTRUMENT IDENTIFICATION NUMBER: Contract N00014-86-K-0366
8c. ADDRESS (City, State, and ZIP Code)	10. SOURCE OF FUNDING NUMBERS: PROGRAM ELEMENT NO.; PROJECT NO.; TASK NO. R&T Code 4134006; WORK UNIT ACCESSION NO.

11. TITLE (Include Security Classification) Universal Detection of IOns by Replacement-Ion Chromatography Employing an Anion-Replacement Method and an Ultraviolet-Visible Spectrophotometric Detector

12. PERSONAL AUTHOR(S) Loenard J. Galante and Gary M. Hieftje

13a. TYPE OF REPORT	13b. TIME COVERED	14. DATE OF REPORT (Year, Month, Day)	15. PAGE COUNT
Technical	FROM ____ TO ____	22 February 1988	40

16. SUPPLEMENTARY NOTATION

Accepted for publication in Analytical Chemistry

17. COSATI CODES		
FIELD	GROUP	SUB-GROUP

18. SUBJECT TERMS (Continue on reverse if necessary and identify by block number) Ion chromatography; Replacement ion chromatography; Chromatographic detectors.

19. ABSTRACT (Continue on reverse if necessary and identify by block number)

A new ion-chromatographic (IC) detection method involving replacement-ion chromatography (RIC) and an anion-replacement arrangement is employed for cation and anion analysis. In the instrument, a conventional dual-column IC system is followed by a continuously regenerated anion-exchange (ionomeric) fiber, which serves as the replacement column. This third column converts all ionic solutes into their iodate or nitrate salts, which are detected sensitively at 215 nm by a UV-visible spectrophotometer. This detection method is especially useful for cation separations, for which the influence of various system parameters are discussed in detail. Good precision (RSD <5%), low detection limits (1-15 ng), and universal calibration were achieved for several monovalent cations. However, the method does not appear to be useful for anion determinations.

20. DISTRIBUTION / AVAILABILITY OF ABSTRACT: [X] UNCLASSIFIED/UNLIMITED [ ] SAME AS RPT [ ] DTIC USERS	21. ABSTRACT SECURITY CLASSIFICATION: Distribution Unlimited
22a. NAME OF RESPONSIBLE INDIVIDUAL: Gary M. Hieftje	22b. TELEPHONE (Include Area Code): (812) 335-2189; 22c. OFFICE SYMBOL

DD FORM 1473, 84 MAR — 83 APR edition may be used until exhausted. All other editions are obsolete.

SECURITY CLASSIFICATION OF THIS PAGE

UNCLASSIFIED

OFFICE OF NAVAL RESEARCH

Contract N14-86-K-0366

R&T Code 4134006

TECHNICAL REPORT NO. 21

UNIVERSAL DETECTION OF IONS BY REPLACEMENT-ION CHROMATOGRAPHY EMPLOYING AN ANION-REPLACEMENT METHOD AND AN ULTRAVIOLET-VISIBLE SPECTROPHOTOMETRIC DETECTOR

by

Leonard J. Galante and Gary M. Hieftje

Prepared for Publication

in

Analytical Chemistry

Indiana University
Department of Chemistry
Bloomington, Indiana 47405

22 February 1988

INTRODUCTION

At present, no completely satisfactory detector exists for quantitating anions and cations by ion chromatography (IC) (1-7). The conductivity detector is the most widely used because of its simplicity and generality. However, it is strongly influenced by temperature; most ionic solutions experience a 2% change in conductivity per °C. Thus, the sensitivity achievable by conductometric-detection methods depends on the ability to minimize background variation caused by temperature fluctuation. Of course, temperature control is more critical when background levels are high. Moreover, detector cells must be well insulated and some are equipped with temperature-compensation circuitry (5,6). Columns and valves can also be environmentally isolated (8).

A number of alternative general detection methods have been investigated for IC. For example, spectroscopic or electrometric methods can be employed after separated ions are reacted with specific reagents. Such post-column derivatization methods have been reviewed (6). Unfortunately, a single post-column reagent cannot often be used for a wide variety of ions; as a result, these methods cannot be considered to be generally applicable.

In the last few years, indirect photometric chromatography has proven to be a competitively sensitive single-column detection method for IC (9-11). In this technique, light-absorbing eluent ions are displaced by nonabsorbing sample ions, which are then measured by a spectrophotometric detector as "trough" peaks in the baseline absorbance. This method has been most extensively employed in anion chromatography with eluents such as phthalate. Detection limits of 1 ng sulfate (9) and 2 ng chloride (10) have been reported. Alkali and alkaline-earth metals have been separated with

Cu^{2+} (9,11) or Ce^{3+} (11) as the eluent cation with detection limits in the range of 8-1200 ng and 0.08-4.0 ng (11), respectively.

A few years ago, a method called replacement-ion chromatography (RIC) was described that allows otherwise species-specific detectors to be used as general detectors for suppressed IC (12). In RIC, a third ion-exchange column called the replacement column is used to replace solute ions (or their co-ions) with another ion (the replacement ion) that can be sensitively monitored by a suitable detector. In the first demonstration of RIC (12), ionic solutes eluting from the suppressor column were converted to their lithium salts by a replacement column containing a cation-exchange resin in the lithium form. Solutes were subsequently detected (indirectly) by monitoring their lithium atomic emission in a hydrogen-air flame.

There are several fundamental advantages to RIC. First, ion replacement allows other desirable detectors to be used as general detectors for IC. More importantly, detectors can be used that are less sensitive to temperature and possibly more sensitive than the conductivity detector. In addition, the integrated detector response of all solutes should be the same in RIC because each solute is stoichiometrically converted into a single detected form. Consequently, RIC is a universal-detection method, and a single calibration curve should apply to all species of the same charge.

In the present publication, we describe an alternative mode of RIC involving anion replacement. Iodate and nitrate were both explored as replacement ions because of their high molar absorptivities at 210 nm (13). Sensitive detection was accomplished with a UV-visible spectrophotometer. We employed a hollow ionomeric anion-exchange fiber (14, 15) as the replacement column because of its low contribution to band broadening and its ability to operate continuously (unlike packed-bed resin columns, which must be regenerated periodically).

In this study, theoretical and experimental guidelines for optimal operation of the fiber-replacement column are discussed. Figures of merit such as sensitivity, detection limits, precision, and dynamic range are evaluated for both cation and anion determinations. The possibility of universal calibration is assessed, and the limitations of the technique are critically evaluated.

EXPERIMENTAL SECTION

Designing an RIC system requires appropriate selection of the replacement ion, replacement column, and detector. Solutes must be exchanged conveniently and efficiently with a replacement ion that can be detected sensitively. Ideally, the detector should be simple and easily interfaced to an ion chromatograph. In the current study, a UV-visible spectrophotometer was chosen; it satisfies adequately these criteria and is also available in most LC laboratories. Furthermore, a number of anions absorb strongly in the UV region near 210 nm (13, 16-18), making them suitable replacement ions. The reported molar absorptivities of iodate and nitrate are 2632 l $mole^{-1}$ cm^{-1} and 9091 l $mole^{-1}$ cm^{-1}, respectively, at 210 nm (13). Iodate and nitrate ions also possess low and moderate resin affinities (7), respectively. Replacement ions that are weakly retained on the ion-exchange sites of the fiber favor efficient and stoichiometric ion exchange. A schematic diagram of the analytical system used for cation determinations is shown in Figure 1.

Equipment

Equipment included an LC pump (model 396 miniPump®, Milton Roy Co., Riviera Beach, FL) and sample-injection valve with a 20-μl sample loop (model 7010, Rheodyne, Cotati, CA). All columns were Dionex products (Dionex Corporation, Sunnyvale, CA). The cation separator column (either CS1, model #30831 or CS2, model #35371) was followed by either a small (CSC-1, model #30832) or large (CSC-2, model #30834) packed-bed cation suppressor column. The anion separator column (AS3, model #30985) was followed by a large packed-bed anion suppressor (ASC-2, model #30828). The replacement column for both anion and cation determinations was a Dionex fiber-suppressor unit (model #35352, including fiber, fiber-housing reservoir, and regenerant reservoir (14, 15)). The fiber is hollow, approximately 2.3 meters long (dry length), and coiled around a support rod in the housing reservoir. The fiber material is proprietary. Columns were connected by 0.3-mm i.d. x 1.6-mm o.d. Teflon tubing with Omnifit (Atlantic Beach, NY) polypropylene tube-end bushings and grippers.

Column effluent was monitored at either 210 or 215 nm by a digital UV-visible spectrophotometer (model GC-55, Perkin-Elmer Corp., Norwalk, CT) modified to perform as an LC detector. The instrument is equipped with a dynamic filter that provides a maximum time constant of one second. Chromatograms were simultaneously traced on a strip-chart recorder (model SR-204, Heath Co., Benton Harbor, MI) and stored on a laboratory computer (MINC-11/23, Digital Equipment Corp., Marlboro, MA) for peak-height or peak-area measurement.

Reagents

Dilute acid solutions were prepared from analytical reagent-grade concentrated nitric acid (Mallinckrodt, Inc., Paris, KY). Sodium hydroxide solutions were prepared by dilution of a 10.0 N volumetric solution (Mallinckrodt, Inc.). The solutions used to maintain the fiber in the IO_3^- or NO_3^- form (regenerant solutions) were prepared from analytical reagent-grade KIO_3 and KNO_3, respectively (Mallinckrodt, Inc.). All other solutions were prepared from analytical reagent-grade (Mallinckrodt, Inc.) or A.C.S. reagent-grade salts (MCB, Cincinnati, OH or Fisher Scientific Co., Fair Lawn, NJ). The water used in all experiments was distilled and deionized.

Procedures

Cation suppressors were regenerated with 0.3 N filtered $Ba(OH)_2$ or 0.1 N NaOH. The anion suppressor was regenerated with 0.35 N HNO_3. Regeneration involved pumping the appropriate solution through the column for at least 30 minutes at a flow rate of 2.0 ml/min. Columns were then rinsed copiously with water.

Regenerant solutions containing 40.0 mN tetramethylammonium hydroxide or potassium hydroxide are recommended for the fiber column when the device functions as an eluent suppressor in cation chromatography (15). Accordingly, solutions containing 40.0 mM of the appropriate replacement ion were initially explored as regenerants for the fiber-replacement column. The fiber was converted into the desired (IO_3^-, NO_3^-, or Cl^-) form by copiously flushing the housing reservoir with a 40.0 mM solution of the respective salt. The fiber was left to soak in this solution for at least 24 hrs. During this time, the housing reservoir was periodically flushed with fresh solution to insure complete conversion. When only the concentration of a regenerant was changed, the fiber was left to equilibrate with the new solution for at least 6 hrs. During operation, the regenerant flow rate through the fiber-housing reservoir was maintained between 2.5-3.5 ml/min countercurrent to column flow and regulated by gravity (15).

Background replacement-ion concentrations in the column effluent were calculated by comparing the background absorbance produced by column effluent to that of standard solutions at 210 or 215 nm.

Void volume and band broadening measurements were made by injecting 20-μl aliquots of 8.0×10^{-4} M KIO_3 both with and without the fiber inserted between the injector and detector cell. Water was used as the eluent at a flow rate of 2.0 ml/min.

RESULTS AND DISCUSSION

Background Replacement-Ion Concentrations in RIC

A finite background replacement-ion concentration arises in RIC from a number of sources including regenerant penetration and contaminant ions. This background concentration causes a corresponding baseline signal upon which analyte peaks are observed. Such a background signal is particularly troublesome if multiplicative noise sources exist within the RIC detection system because they cause fluctuation in an otherwise stable background signal. In such a situation, detection limits are degraded in proportion to both the multiplicative noise and the <u>magnitude</u> of the background signal. Consequently, background levels and their dependence on operating conditions were assessed in the present system. This information can be used also to predict the attractiveness (e.g., detection limits) of alternative replacement-anion/detector combinations.

Regenerant Penetration. Ideally, the cations in the inner (chromatographic) and outer (regenerant) flow streams are selectively excluded from the fiber by the Donnan potential of the fiber pores, and only the anions can pass through the fiber wall during the exchange process. However, at high regenerant-ion concentrations, this potential is exceeded by the strong concentration gradient across the fiber. As a result, both anions and cations in the regenerant can penetrate the fiber and enter the inner flow stream. The permeation rate depends principally on the size, charge, and concentration of the co-ion and upon fiber characteristics (15, 19-21). A regenerant salt and concentration should be chosen that provides adequate exchange but minimal background from regenerant penetration.

Figure 2 shows the background replacement-ion concentration that results from 40.0 mM KIO_3 (*, curve A) and KNO_3 (◎, curve B) regenerant solutions over a range of eluent (distilled water) flow rates. The unusually high background level and its strong dependence on pump rate indicate that background is caused principally by the penetration of regenerant ions through the fiber wall. Under this condition, background replacement-ion concentration is inversely proportional to pump rate (21). Linear-regression analysis of the data provides a good fit to the function $y = B/X + A$ where X is the pump rate and y is the observed background. For KIO_3, $B = (3.59 \pm 0.04) \times 10^{-9} \frac{\text{moles}}{\text{sec}}$, $A = (3.04 \pm 0.26) \times 10^{-5}$ M, the square of the correlation coefficient $(r^2) = 0.999$, and the standard error of estimate (SEE) $= 4.04 \times 10^{-6}$. For KNO_3, $B = (3.17 \pm 0.02) \times 10^{-9} \frac{\text{moles}}{\text{sec}}$, $A = (2.75 \pm 0.14) \times 10^{-5}$ M, $r^2 = 1.00$, and the SEE $= 1.82 \times 10^{-6}$. The coefficients, B, are the empirically derived permeation rates of KIO_3 and

KNO_3 through the fiber at a regenerant concentration of 40 mM. The equations are displayed in Figure 2 as curves A and B, respectively.

Regenerant penetration is a relatively unimportant background source at high pump rates or lower regenerant concentrations. As shown in Figure 2 (dotted lines C and D), decreasing the regenerant concentration from 40.0 mM to 4.0 mM results in a dramatic drop in background concentration for both the IO_3^- and NO_3^- fibers. Moreover, the background concentration is then relatively insensitive to flow rate.

When the regenerant concentration is decreased further from 4.0 to 0.4 mM, background decreases by only another 15-20% over the flow rate range shown in Figure 2 and reaches an average value of about 2.4×10^{-5} M for both fibers. This background level persists even if the regenerant solution is replaced by distilled water, which suggests that a residual background component exists in the absence of significant regenerant penetration. This conclusion is supported also by the magnitude of the intercepts in the equations derived above for the 40.0 mM regenerant.

Contaminant Sources. This residual background component (~ 2.0×10^{-5} M) appears to be caused by a number of contaminant sources. Measurements by inductively-coupled plasma emission spectrometry suggest that less than 10% of the background replacement-ion concentration could be caused by ionic impurities (mostly Na^+, Ca^{2+}, and Mg^{2+}) in our laboratory water. However, low levels of additional contaminant ions can be introduced by metallic chromatographic components that contact the flowing liquid. In addition, the pH of our laboratory water is typically between 5.5 and 6.0 because of dissolved CO_2. Dissolved CO_2 introduces an additional ionic impurity, HCO_3^-.

To verify that the residual background absorbance is caused by the exchange of contaminant ions with the replacement ion and not by a light-absorbing contaminant (e.g., an organic absorber leaching from the fiber), a nonabsorbing replacement ion was employed. Chlorine ion was chosen because it absorbs negligibly at 215 nm or 210 nm compared to NO_3^- or IO_3^-. With the fiber in the Cl^- form, the relative background absorbance of the column effluent dropped to nearly zero, suggesting that the background signals measured previously with the NO_3^- or IO_3^- fiber were indeed caused by the exchange of contaminant ions with the corresponding replacement ion.

Optimal Operating Conditions and Exchange Efficiency of the Fiber-Replacement Column

The ion-exchange efficiency of a fiber column is affected by a number of parameters, including the influent ion concentration, regenerant concentration and flow rate, fiber length, and column-flow rate (21). The influence of these parameters on the performance of the fiber-replacement column is discussed below.

Effect of Regenerant Flow Rate and Concentration. When the fiber column is employed as a suppressor column in conventional IC, it must continuously exchange millimolar concentrations of eluent ions. Accordingly, high regenerant flow rates and concentrations are often required. In contrast, the demands on the fiber are lower when it is used as a replacement column in RIC, because the fiber need exchange only solute ions, which elute discontinuously and experience considerable dilution during the separation. Consequently, regenerant flow rate and concentration have little effect on replacement-column performance and can be varied over a wide range. Flow rates in the range of 2.5-3.5 ml/min provide satisfactory performance.

The influence of regenerant strength on signal magnitude and reproducibility in RIC was investigated by injecting successive 20-μl aliquots of 10.0 mM NaOH (a realistic upper-limit concentration encountered in IC) into the fiber-replacement column bathed with a 40.0 mM, 4.0 mM, and 0.4 mM KIO_3 regenerant solution. NaOH was chosen because separated cations elute from the suppressor column and enter the fiber column as hydroxides in RIC (Figure 1). The peak heights and standard deviations obtained from these injections were compared with those produced by 10.0 mM KIO_3 (IO_3^- does not require ion-exchange). The eluent (distilled water) flow rate was 2.0 ml/min. The NaOH and KIO_3 solutions produced an equivalent (0.5% RSD) peak-height response at all regenerant concentrations. These data suggest that the analyte response is independent of regenerant concentration and that the fiber quantitatively converts NaOH to $NaIO_3$ within the accuracy of this measurement procedure.

Based on the foregoing discussion, the best signal-to-background ratios in RIC are obtained when the replacement column is bathed with regenerant solutions dilute enough to preclude ion penetration but sufficiently concentrated to prevent contaminant ions from concentrating on the fiber and competing with regenerant ions. A 4.0 mM regenerant concentration appears to be an acceptable compromise. With the UV-visible spectrophotometer, the baseline noise was similar when either a 4.0 or 40.0 mM regenerant concentration was employed, despite the much greater background produced by the latter. However, this insensitivity of baseline noise to background might not be observed for other detectors, particularly those more susceptible to multiplicative noise sources. In such cases, lower regenerant concentrations (e.g., 4.0 mM) would provide better signal-to-noise ratios. Alternatively, a regenerant co-ion less permeable to the fiber wall than potassium could be employed (15, 19).

Fiber Length. Long fibers are required to continuously exchange concentrated solutions because the mass transport of ions through the fiber wall limits the rate of ion-exchange. In RIC, where the average influent ion concentration is low and noncontinuous, this process is unimportant because the ion-exchange sites of the fiber-replacement column are less likely to saturate and the inner wall acts like a perfect sink to ions requiring exchange. Under this condition, ion-exchange efficiency is limited by the transport of ions to the inner wall of the fiber and an exponential relationship exists between fiber length (L) and the fraction of ions (f) that are exchanged (21). For a linear, hollow fiber under laminar-flow conditions, the relationship is approximated by the Gormley-Kennedy equation (21):

$$1-f = 0.8191e^{-3.657\pi DL/F} + 0.0975e^{-22.3\pi DL/F} + 0.0325e^{-57\pi DL/F} \qquad (1)$$

In equation 1, D is the diffusion coefficient of the ion being exchanged and F is the flow rate of the eluent.

Equation 1 can be used to predict the length of fiber required in the replacement column for the efficient exchange of solutes in cation analysis. Here, separated cations enter the replacement column as hydroxides (Figure 1), so the diffusion coefficient of OH^- ion, 5.26×10^{-9} m^2/s at 25°C (22), is applicable. At 2.0 ml/min, 3.0- and 2.0-m fibers would be required for exchange efficiencies of 99.6% and 97.8%, respectively.

Actually, the length required for a particular exchange efficiency might be somewhat shorter than that predicted by equation 1 because of pump pulsations, turbulence caused by fiber-surface roughness, and other factors that enhance mass transport and increase exchange efficiency (21). Also, fibers are ordinarily coiled around a support rod and are sometimes packed with beads (23, 24) or filaments (21, 25-27). These modifications promote convective radial transport of ions to the walls and cause even greater departures from the simple theoretical model presented above for linear, hollow fiber devices.

In the current RIC system, a 2.3-m fiber was employed and provided adequate exchange efficiency for our application. Injections of NaOH into the IO_3^- fiber (previously discussed) had verified that OH^- is stoichiometrically replaced by IO_3^-. The quantitative replacement of OH^- by NO_3^- (with a 4.0 mM KNO_3 regenerant) was also verified for a 0.4 mM NaOH solution that was pumped continuously through the fiber and detector cell at 2.0 ml/min; the absorbance of the column effluent was experimentally indistinguishable from that of 0.4 mM KNO_3. This result is consistent with equation 1; replacement efficiency depends upon the diffusion coefficient of the ion to be replaced (OH^-) but not upon the identity of the replacement ion. However, one might expect that if the affinity of the fiber for the replacement ion were dramatically greater than its affinity for OH^-, the fiber would behave less like a perfect sink for OH^- ions. Consequently, ion-exchange efficiency would decrease and longer fibers would be required. In the extreme, ion-exchange efficiency would be minimal for a replacement ion that was irreversibly adsorbed onto the exchange sites.

Detector Evaluation

Peak-to-peak noise levels of 1.5×10^{-4} absorbance units (AU) were measured at 215 nm with the detector cell filled with distilled water. The absolute detection limits (S/N = 3) for IO_3^- and NO_3^- ion were calculated to be 5.5×10^{-7} M and 2.0×10^{-7} M, respectively, based on the net absorbances produced above that of water by 8.0×10^{-5} M standard solutions of the ions. When detection at 210 nm was investigated, signal levels increased by a factor of 1.3 to 1.4, but noise levels increased proportionately. At 215 nm, the detector response became nonlinear at concentrations above 2×10^{-3} M and 8×10^{-4} M for IO_3^- and NO_3^- ion, respectively, thereby defining the absolute upper limit of linearity. The linear dynamic range is therefore approximately 10^4 for both anions.

Cation Determinations by RIC

Working Curves and Dynamic Range. The dynamic range was investigated for cations by injecting lithium concentrations between 10^{-4} and 10^{-1} M into the system shown in Figure 1. (Three injections were made at each concentration.) The portion of the peak-height calibration curve that provides the best linear fit extends from at least the lowest injected concentration, 1.0×10^{-4} M, to about 5.0×10^{-3} M. Linear regression analysis of the data points in this concentration range provides the equation: y[peak height] = 77,300 C[Li^+ concentration (M)] -2.12 (r^2 = 1.00 and SEE = 1.01). Peak heights at greater concentrations deviate negatively from those predicted by this equation because the column's sample capacity is exceeded. For example, the response at 1.0×10^{-2} M is low by 5-6%. The degree of deviation increases progressively at injected concentrations above 10^{-2} M.

In contrast, the linear dynamic range extends well beyond 1.0×10^{-2} M when peak area is measured; up to 10^{-2} M, y[peak area] = 1140 C[Li^+ concentration (M)] -0.021 (r^2 = 1.00 and SEE = 0.0264). At concentrations approaching 0.1 M, peak areas begin to deviate from this equation because the detector response no longer obeys Beer's law. However, the effect is usually minor because peak heights no longer increase proportionately at concentrations that exceed the column's sample capacity. For example, the area response at 0.1 M is low by only 1.7%.

Interestingly, both calibration equations presented above have small negative intercepts, a feature common to all RIC working curves generated in this study. We believe these negative intercepts occur because the relationship between RIC response and injected concentration is slightly nonlinear. Based on unweighted least-squares analysis of the accumulated data, the exponential function, $y = AX^B$ (where B usually equals 1.02 or 1.03 and A is a constant), often provides a similar (R^2 also equals 1.00) or slightly better fit (lower standard error of estimate) than a linear equation with a negative intercept.

The cause of this slightly nonlinear response is not certain but appears to be linked to the replacement column. The effect of the fiber column on signal recovery was evaluated by injecting KNO_3 into the detector cell with and without the fiber column (NO_3^- form) inserted between the injector and detector. The results are shown in Table I. The peak heights obtained without the fiber (second column in Table I) are linear with respect to concentration. Least-squares analysis indicates that the data fit best a line passing through the origin or a line having a slightly positive intercept. In both cases $r^2 = 1.00$, but the latter provides a slightly lower standard error of estimate.

The peak heights obtained with the fiber in place (Table I, column 3) should be lower by a constant percentage than those measured without the fiber because of the fiber's void volume. Instead, the percent recovery of the signal (Table I, column 4) increased as the injected ion concentration increased. Least-squares analysis indicates that the best linear fit for the peak heights in column 3 of Table I produces a small negative intercept with $r^2 = 1.00$. Moreover, the function $y = AX^B$ where $B = 1.09$ provides a slightly better fit ($r^2 = 1.00$ and lower standard error of estimate).

The reason for the observed influence of the fiber on analyte response is not clear. However, nonlinearity at low concentrations in IC is not a problem unique to RIC. Calibration curves in dual-column IC are also frequently nonlinear at the low-concentration end and do not typically intersect the conductance axis at the origin (7, 25). The nonlinear response has been attributed to interactions between the suppressor-column effluent and the eluted ion (7) or the inability of fiber suppressors to be 100% efficient (25). Even very efficient devices (> 99.90% suppression) pass μM amounts of unsuppressed eluent ions that appear to interfere with the detection of sample ions at low injected concentrations (25).

Reproducibility. The relative standard deviation of peak-height measurements for lithium was 5% or better for injected concentrations $\leq 2 \times 10^{-4}$ M and 1% or lower in the concentration range between 5×10^{-4} M and 10^{-1} M. The relative standard deviation of peak-area measurements for lithium varied between 0.3% and 4.0%.

Detection Limits. Five successive 20-μl injections of 1×10^{-4} M (0.7 ppm) Li^+ yielded a mean signal-to-background noise ratio of 40, with IO_3^- as the replacement ion. This injection, corresponding to an absolute mass of 14 ng Li^+, produces an extrapolated detection limit (S/N = 3) at a 99.9% confidence level (28) of 1.1 ng. The detection limits for Na^+, NH_4^+, and K^+ are 5.0 ng, 6.0 ng, and 15 ng, respectively.

The detection limits quoted above necessarily assume that the RIC working curve is linear at low analyte concentrations and passes through the origin. However, the data and discussion presented earlier revealed that the exponential function, $y = AX^B$, might be even more accurate, particularly at low analyte concentrations. Accordingly, the lithium detection limit was calculated also by converting the lithium peak heights to signal-to-noise ratios and extrapolating to S/N = 3 using the best least-squares fit of the data to this function. This approach yields a detection limit for lithium of 1.2 ng, nearly the same as the value obtained by linear extrapolation (1.1 ng).

Sensitivity and detection limits should improve by employing a replacement ion of greater molar absorptivity. As illustrated in Figure 3, the signal-to-baseline noise ratio of a 14 ng Li^+ injection increased by a factor of about 2.2 when NO_3^- was substituted for IO_3^- as the replacement ion under otherwise identical experimental conditions. The extrapolated detection limit for Li^+ detected as $LiNO_3$ is correspondingly lower (0.5 ng).

Universal Calibration. The universality of the method was evaluated for Li^+, Na^+, NH_4^+, and K^+ by peak-area integration. Three to four injections were made of each ion at concentrations between 8×10^{-4} M and 8×10^{-3} M. Each synthetic sample contained only two components, consisting of either Li^+ and NH_4^+ or Na^+ and K^+, in order to eliminate the possibility of peak overlap or solute interaction, and to simplify peak-area integration. The relative standard deviation of peak areas for the individual ions varied from less than 4% at lower concentrations to less than 2% at higher concentrations.

Table II summarizes the best least-squares linear fit of the data and verifies that the integrated detector response can be considered to be universal; the agreement among Li^+, Na^+, and K^+ is excellent. The slope of the NH_4^+ working curve is slightly lower by about 2-3% than those of the other cations.

The slightly different response for NH_4^+ is not at first surprising. In conventional dual-column IC, the working curve of NH_4^+ is not linear but deviates negatively at high concentrations, which complicates the determination of this ion (6, 29). Nonlinearity occurs because the ion forms NH_3 in the suppressor column, which is only partially ionized in the conductivity detector cell. For example, a 0.4 mM solution of NH_3 in water is only 19% ionized, based on the base-dissociation constant, K_b, of NH_3 at 25°C (30). In contrast, the RIC working curve of NH_4^+ (Table II) is linear. Moreover, the magnitude of the slope is much greater than would be predicted from the fractional ionization of NH_4OH. The enhanced ionization of NH_3 can be explained by a dynamic equilibrium effect that occurs in the third (replacement) column (29). The pertinent equilibrium reaction is:

$$NH_3(aq) + H_2O \underset{2}{\overset{1}{\rightleftarrows}} NH_4^+(aq) + OH^-(aq)$$

As the NH_3 passes through the replacement column and OH^- ion is exchanged (replaced) with IO_3^-, the above reaction is continually shifted towards the formation of NH_4^+ from NH_3 to replenish the depleted OH^- concentration.

The integrated response of NH_4^+ did not appear to deviate more severely from those of the other cations at higher concentrations but varied consistently by 1.6-2.9%. The lower response might be caused by incomplete conversion of NH_3 to NH_4IO_3. Alternatively, incomplete exclusion of the solute by the Donnan potential of the suppressor-column resin or of the fiber ionomer might be responsible. The partially neutral character of NH_4OH allows it to penetrate these materials more extensively than do the hydroxides of the other cations. Increased penetration could result in signal losses via several mechanisms including the adsorption of NH_3 by the suppressor-column resin (5) or the diffusion of NH_3 through the wall of the fiber.

Incomplete exclusion is known to be serious for NH_4^+ ion when packed-bed suppressor columns are employed in conventional IC; retention times, peak heights and, in some cases, peak areas are strongly influenced by the degree of exhaustion and by the type of the suppressor column (5, 29). Solute adsorption in the large packed-bed suppressor column used in the present RIC experiments might be primarily responsible for the lower integrated response of NH_4^+. The RIC response of NH_4^+ would probably agree more closely to those of the other cations if the suppressor column were replaced with a fiber device.

Nevertheless, the results in Table II show that for many applications, only one calibration curve or standard is required in RIC. In addition, in applications where only the relative molar amounts of various cations are important, standard calibration is not even required. For example, Figures 4A and 4B each show a representative chromatogram of a synthetic sample containing Li^+, Na^+, NH_4^+, and K^+. The mean peak-area response of each cation after six replicate injections appears in parentheses. The peak areas indicate that Li^+ and K^+ are present at twice the molar concentration (1.0×10^{-3} M) of Na^+ and NH_4^+ (5.0×10^{-4} M) in Figure 4A but that species are present at equal concentrations (5.0×10^{-4} M) in Figure 4B.

These chromatograms demonstrate the ability of RIC to perform quantitative analysis without prior identification of sample ions. For example, in the chromatogram of Figure 4B, it is apparent that all the monovalent ions, regardless of identity, are present at a relative normal concentration of about 25% with respect to the total ion concentration of the sample. The relative normal concentration of an unknown ion could be determined in a similar fashion.

Two single-column IC methods possess this same capability. Wilson, Yeung, and Bobbitt have shown that solutes can be quantitated without prior identification with errors less than a few percent when either a conductivity or absorbance detector is employed (31, 32). This novel method, not applicable only to IC, requires measurement of the area response produced by the analyte when two different eluents are employed and requires solving several equations simultaneously. The procedure suffers from the disadvantage that two individual chromatograms are needed and that the analyte ion must produce a significantly different response when separated by the two eluents. Although the method is conceptually interesting, it could be difficult to implement in practice.

Indirect photometric chromatography also provides universal detection capability without identification. However, that technique possesses its own intrinsic disadvantages. Ion detection and separation are interrelated because both are accomplished via the eluent. Consequently, conditions that provide optimal sensitivity or chromatographic resolution might not be the same (9-11, 33). Furthermore, one must assume that only the eluent and not the analyte absorbs at the selected absorption wavelength. This information would not be available for an unknown ion.

In each of the universal calibration methods discussed above, the analyte's signal is proportional to charge. This is true also of RIC. For example, a divalent cation produces twice the signal of a monovalent cation because it co-elutes with two replacement anions. The doubling of analyte signal for doubly-charged cations in RIC was verified here by injecting 2.0×10^{-4} M KCl and 2.0×10^{-4} M $BaCl_2$ directly into the fiber-replacement column (NO_3^- form). As expected, the mean peak-height response for $BaCl_2$ was twice that produced by KCl within 1.0%. Accordingly, the charge of an unidentified ion must be determined by varying the eluent concentration and measuring the ion's retention time (9, 32) before it can be quantitated.

Anion Determinations

The determination of anions was investigated using equipment analogous to that shown in Figure 1 but with the appropriate separator and suppressor columns. Unfortunately, unusually poor sensitivity, peak shape, and reproducibility were encountered for this RIC mode, in contrast to that obtained for the detection of cations. To further characterize the influence of the third column on the analyte signal, solutions of KIO_3 between 0.16 mM and 4.0 mM were injected into the RIC instrument. Sample chromatograms appear in Figure 5A. Injections were made also in the absence of the replacement column but under otherwise identical experimental conditions. Sample chromatograms resulting from the injection of 0.4 mM and 0.16 mM KIO_3 appear in Figure 5B.

<u>Sensitivity</u>. When the dual-column system (no solute replacement) was employed, iodate ion was sensitively detected and peak heights were proportional to concentration (Figure 5B). However, the peak heights decreased dramatically when the replacement column was added (Figure 5A).

Moreover, peak heights were not proportional to concentration. Instead, peak heights generally increased more than proportionately as concentration increased.

<u>Peak Shape</u>. The RIC peaks in Figure 5A are unusually asymmetrical and unlike those obtained without the replacement column in place (Figure 5B); the leading edge is sharp, and there is significant tailing before the peak returns to baseline. This severe tailing obviously accounts at least partially for the abnormally low peak heights shown in Figure 5A. The peaks of F^-, Cl^-, and Br^- were likewise poorly shaped when they were detected by RIC (with the replacement column in place). Peak asymmetry was most noticeable for F^- but less so for the later-eluting peaks (Cl^- and Br^-). This severe peak tailing seriously degraded resolution when mixtures of these ions were injected.

<u>Reproducibility</u>. Peak-height reproducibility for anions was measurably worse by RIC than by dual-column IC. Relative standard deviations (RSDs) for 2-3 <u>consecutive</u> injections of IO_3^- at the higher concentrations shown in Figure 5A were about 2% with the tri-column system but about 0.5% with the dual-column system. The RSDs for 2.0 mM F^-, 2.0 mM Cl^-, and 2.0 mM Br^- injected as a synthetic mixture and detected by RIC were 5.6%, 0.3%, and 2.0%, respectively.

The long-term reproducibility of the tri-column system was particularly poor. For example, the mean peak-height response of a 1.6 mM IO_3^- injection increased by about 40% after the system was operated continuously for 1.5 hrs and after several anion species were injected at various concentrations. The width of the peak base decreased correspondingly. Day-to-day peak-height response varied considerably, sometimes by as much as 50%. The response changed dramatically also when different suppressor columns were employed. The reason for these variations is not yet clear.

Universal Calibration. Conceptually, a universal peak-area response should exist for all anions at the same concentration. However, a quantitative comparison was not pursued here because of the poor reproducibility and peak tailing that were encountered. The severe tailing made it difficult to accurately define peak baselines or to obtain adequate resolution for multi-component samples. Consequently, even if a universal detector response exists for anions, it cannot be practically exploited in this anion-replacement RIC method.

Interactions in the Replacement Column. The low sensitivity, poor peak shape, and irreproducibility seem to arise because the separated anions enter the replacement column as their conjugate acids after passing through the anion suppressor column. The effect of the replacement column is illustrated in Figure 6, which compares the detector response produced by 0.01 M KIO_3, NaOH, NaCl, and HCl injected directly into the fiber-replacement column. Again, the fiber was in the IO_3^- form. An alkali hydroxide, in this case NaOH, represents the chemical form in which cations enter the replacement column during cation analysis. The strong acid, HCl, represents the chemical form in which anions enter the replacement column when anion analysis is performed. The neutral salt, NaCl, was introduced for comparison. The sodium salts of OH^- and Cl^- reproducibly generated a nearly identical response to that of KIO_3. In contrast, HCl yielded a far lower peak signal and also exhibited much greater tailing. In addition, the peak-height response was not as reproducible as those produced by the other solutions and usually increased slightly with each successive injection of HCl. Similar results were observed when HNO_3 was injected into the fiber column (in its NO_3^- form).

We believe that acids (cf. HCl in Figure 6) are being partially absorbed by the fiber ionomer because they are incompletely excluded from the fiber pores. As discussed earlier, anions pass easily through the fiber pores and are ion-exchanged, whereas cations are comparatively excluded, especially those that are large and multi-charged (19). Among cations, the proton should pass most easily through the fiber pores because of its small size and charge. Moreover, diffusion of protons through the fiber wall might be exacerbated because the fiber imbibes water. The diffusion of HNO_3 through the fiber was compared to that of KNO_3 by pumping distilled water through the fiber (NO_3^- form) and measuring the background NO_3^- concentration in column effluent. Both a 40.0 mM HNO_3 and 40.0 mM KNO_3 regenerant solution were tested. The background NO_3^- concentration produced by the 40.0 mM HNO_3 regenerant solution was 4.6 times greater than that produced by the KNO_3 solution at a flow rate of 2.0 ml/min. These data suggest that the diffusion rate of H^+ (as HNO_3) in the fiber material is 4.6 times greater than that of K^+ (as KNO_3).

Better success with anion determinations might be obtained if the fiber were fabricated from a different ionomer. Recently, Dasgupta (34) evaluated the performance of several types of anion-exchange membranes that permit the sensitive determination of anions by postsuppression ion exchange chromatography, identical in concept to the original RIC (12). Several detection modes were investigated by using anthranilate, a fluorescent and optically absorbing anion, as the replacement ion with no apparent problem from unusual peak tailing (34). Alternatively, anions can be detected by RIC utilizing a cation-replacement method (12, 34, 35).

Limitations of RIC

RIC possesses a number of inherent liabilities that cannot be eliminated. The addition of a third column clearly increases the complexity of IC instrumentation, although the use of a fiber-replacement column minimizes the disadvantage. Also, peak-area integration is necessary to exploit the universal calibration feature of RIC. Peak-area determinations require an integrator or computer and adequate chromatographic resolution. However, the third column also degrades chromatographic resolution and increases retention times. Fortunately, the fiber void volume is small, measured here to be only 218 μl. Accordingly, peak retention times increase only 6-7 seconds at a flow rate of 2.0 ml/min.

The band broadening introduced into the IC system by the fiber column was studied by measuring peak widths at half height with and without the fiber inserted between the injector and detector. For simplicity, the peaks were assumed to be Gaussian in shape, and their base widths taken to be twice the width at half height, which corresponds to 4.7 σ (4.7 σ includes 98% of the area of a Gaussian profile). The fiber's contribution to peak width, V_F, was then determined from equation 2 (36).

$$(V_W)^2 = (V_{WO})^2 + (V_F)^2 \qquad (2)$$

In equation 2, V_{WO} is the width of the peak without the fiber and V_W is the width of the peak with the fiber. From this relation, V_F was calculated to be 75 μl at 2.0 ml/min.

The relative increase in peak width of an RIC system over that of a conventional-dual column system can be predicted from equation 2 rearranged into the following form (36):

$$\frac{V_W}{V_{WO}'} = \left[1 + \left(\frac{V_F}{V_{WO}'}\right)^2\right]^{1/2} \qquad (3)$$

In this case, V_{WO}' is the peak width observed in dual-column IC.

It is evident from equation 3 that the relative increase in peak width will be worse for early-eluting peaks or peaks separated by very efficient columns (small V_{WO}'). Because peak widths in IC are relatively large, there is relatively little influence of added void volume before the detector. For example, a peak eluting in dual-column IC with a base width of 0.5 ml and with $V_F = 75$ µl should broaden by only 1% when the fiber is added.

Importantly, the value of V_F stated above should be regarded as a conservative estimate of the band broadening introduced by the fiber, because only symmetrical band broadening has been considered; any tailing that might result from added dead volume has been ignored. Moreover, the determination of V_F has assumed that the eluting peaks are Gaussian. In fact, the peaks obtained by this flow-injection procedure were somewhat asymmetric. The long time constant, 1 sec, of the spectrophotometric instrument might be partially responsible for the asymmetric peak profiles. A time constant of 0.3 sec would have been more appropriate for these measurements, based on the standard deviation of the observed peaks (36).

CONCLUSIONS

The detection method described is not only general but also universal and clearly applicable to the determination of alkali metals and NH_3. Detection limits (absolute mass) are similar to those reported earlier for dual-column IC with conductometric detection (7), but are more than an order of magnitude larger than those recently reported for cations detected by indirect photometric chromatography (11, 37). We are currently exploring alternative replacement-ion/detector arrangements that will potentially provide lower detection limits.

Although not demonstrated in the present paper, this RIC method should be applicable to the sensitive determination of alkylamines (29) with the potential advantage of providing linear working curves not offered by dual-column IC with conductometric detection. RIC should be useful also for the determination of alkaline-earth ions and Ni^{2+} (5). These cations were not chromatographically separated and detected by RIC in the present study because the recommended eluent contains millimolar amounts of m-phenylenediamine (m-PDA). M-PDA absorbs strongly at 210 and 215 nm, so the detector would not be able to sensitively discriminate between absorbing eluent and solute species. An alternative eluent or replacement-ion/detector scheme insensitive to m-PDA is required.

ACKNOWLEDGEMENT

We are grateful to Milos V. Novotny for the loan of the UV-visible spectrophotometer employed in this study and to Dionex Corporation for providing the chromatographic columns.

CREDIT

Supported by the National Science Foundation through grant CHE 83-20053, by the Office of Naval Research, by American Cyanamid, and by Monsanto.

REFERENCES

1. Small, H.; Stevens, T. S.; Bauman, W. C. Anal. Chem. **1975**, 47, 1801-1809.
2. Gjerde, D. T.; Fritz, J. S.; Schmuckler, G. J. Chromatogr. 1979, 186, 509-519.
3. Gjerde, D. T.; Schmuckler, G.; Fritz, J. S. J. Chromatogr. **1980**, 187, 35-45.
4. Fritz, J. S.; Gjerde, D. T.; Becker, R. M. Anal. Chem. **1980**, 52, 1519-1522.
5. Pohl, C. A.; Johnson, E. L. J. Chromatogr. Sci. **1980**, 18, 442-452.
6. Fritz, J. S.; Gjerde, D. T.; Pohlandt, C. Ion Chromatography; Dr. Alfred Hüthig Verlag: Heidelberg, West Germany, 1982.
7. Smith, F. C., Jr.; Chang, R. C. The Practice of Ion Chromatography; John Wiley & Sons: New York, 1983.
8. Johnson, E. L. Am. Lab. February **1982**, 98-104.
9. Small, H.; Miller, T. E., Jr. Anal. Chem. **1982**, 54, 462-469.
10. Naish, P. J. Analyst **1984**, 109, 809-812.
11. Sherman, J. H.; Danielson, N. D. Anal. Chem. **1987**, 59, 490-493.
12. Downey, S. W.; Hieftje, G. M. Anal. Chim. Acta **1983**, 153, 1-13.
13. Buck, R. P.; Singhadeja, S.; Rogers, L. B. Anal. Chem. **1954**, 26, 1240-1242.
14. Slingsby, R. W.; Riviello, J. M. LC Mag. **1983**, 1(6), 354-356.
15. Dionex Product Document No. 032244.
16. Williams, R. J. Anal. Chem. **1983**, 55, 851-854.
17. Reeve, R. N. J. Chromatogr. **1979**, 177, 393-397.
18. Leuenberger, V.; Gauch, R.; Rieder, K.; Baumgartner, E. J. Chromatogr. **1980**, 202, 461-468.

19. Dasgupta, P. K.; Bligh, R. Q.; Lee, J.; D'Agostino, V. Anal. Chem. 1985, 57, 253-257.

20. Hanaoka, Y.; Murayama, T.; Muramoto, S.; Matsuura, T.; Nanba, A. J. Chromatogr. 1982, 239, 537-548.

21. Dasgupta, P. K. Anal. Chem. 1984, 56, 96-103.

22. Atkins, P.W. Physical Chemistry; W. H. Freeman and Company: San Francisco, CA, 1978; Chapter 25.

23. Stevens, T. S.; Jewett, G. L.; Bredeweg, R. A. Anal. Chem. 1982, 54, 1206-1208.

24. Stevens, T. S. Ind. Res. Dev. September 1983, 96-99.

25. Dasgupta, P. K. Anal. Chem. 1984, 56, 103-105.

26. Dasgupta, P. K. Anal. Chem. 1984, 56, 769-772.

27. Dasgupta, P. K.; Bligh, R. Q.; Mercurio, M. A. Anal. Chem. 1985, 57, 484-489.

28. St. John, P. A.; McCarthy, W. J.; Winefordner, J. D. Anal. Chem. 1967, 39, 1495-1497.

29. Bouyoucos, S. A. Anal. Chem. 1977, 49, 401-403.

30. Brown, T. L.; LeMay, H. E., Jr. Chemistry: The Central Science; Prentice-Hall: Englewood Cliffs, NJ, 1977; p 467.

31. Wilson, S. A.; Yeung, E. S. Anal. Chim. Acta 1984, 157, 53-63.

32. Wilson, S. A.; Yeung, E. S.; Bobbitt, D. R. Anal. Chem. 1984, 56, 1457-1460.

33. Jenke, D. R. Anal. Chem. 1984, 56, 2468-2470.

34. Dasgupta, P. K.; Shintani, H. Anal. Chem. 1987, 59, 1963-1969.

35. Galante, L. G.; Hieftje, G. M., Anal. Chem. 1987, 59, 2293-2302.

36. Snyder, L. R.; Kirkland, J. J. Introduction to Modern Liquid Chromatography, 2nd ed.; John Wiley & Sons: New York, 1979; pp 31-33, 130.

37. Sherman, J. H.; Danielson, N. D. Anal. Chem. 1987, 59, 1483-1485.

Table I. Mean Peak-height Response[a] Produced by Several KNO_3 Solutions with and without the Fiber Column[b] Preceding the Detector Cell.

Injected KNO_3 Concentration (mM)	Mean Peak Height without Fiber (Arb. Units)	Mean Peak Height with Fiber (Arb. Units)	Signal Recovery with Fiber[c] (%)
0.08	23.1	16.0	69.3
0.16	46.3	35.0	75.7
0.40	115	94.9	82.4
0.80	226	199	88.2

[a]Determined by six or more 20-μl injections eluted with distilled water at 2.0 ml/min and detected at 215 nm.

[b]Fiber bathed with a 4.0 mM KNO_3 solution flowing at 3.4 ml/min.

[c]Calculated as the ratio of the peak heights obtained with and without the fiber column (multiplied by 100).

Table II. Least-Squares Linear Fit of Peak-Area Calibration Curves for Several Cations[a].

Cation	Least-Squares Slope	Least-Squares Intercept ($\times 10^2$)	Correlation Coefficient	Standard Error of Estimate
Li^+	1089 ± 4	-4.87 ± 1.62	1.00	0.0230
Na^+	1085 ± 4	-4.03 ± 1.65	1.00	0.0234
NH_4^+	1052 ± 3	-2.61 ± 1.27	1.00	0.0181
K^+	1078 ± 6	-4.95 ± 2.31	1.00	0.0328

[a]Replacement ion, IO_3^-. Fiber-column regenerant, 40.0 mM KIO_3. Detection wavelength, 215 nm. Eluent, 10.0 mN HNO_3. Flow rate, 2.2 ml/min. Sample size, 20 µl. Concentration range, 8×10^{-4} to 8×10^{-3} M.

Figure Captions

Figure 1. Schematic diagram of RIC system used for cation determinations using IO_3^- as the replacement ion. Here, the fixed charge (either R^+ or R^-) and the counter ion of each column are shown. The ions associated with the separated cations (M^+) as they exit each column are shown also.

Figure 2. Variation of background replacement-ion concentration with pump rate using either IO_3^- (*, curves A and C) or NO_3^- (⊙, curves B and D) as the replacement ion. Background levels obtained with a 40.0 mM regenerant solution (solid curves, A and B) and 4.0 mM regenerant solution (dotted curves, C and D) are shown. Eluent, distilled water.

Figure 3. Chromatograms illustrating the signal-to-noise ratio for injections of 14 ng Li^+ with the fiber-replacement column conditioned in A) the IO_3^- form and B) the NO_3^- form; fiber bathed with 40.0 mM KIO_3 and 40.0 mM KNO_3, respectively, flowing at 3.0 ml/min. Otherwise, both chromatograms were obtained under identical conditions. Columns, CS1 separator and CSC-2 suppressor; eluent, 7.0 mM HNO_3, pumped at 2.0 ml/min; sample, 1.0×10^{-4} M Li^+; injection volume, 20 μl; detector wavelength, 215 nm.

Figure 4. Chromatogram illustrating the response produced by a synthetic mixture containing A) 1.0×10^{-3} M Li^+, 1.0×10^{-3} M K^+, 5.0×10^{-4} M Na^+ and 5.0×10^{-4} M NH_4^+ and B) 5.0×10^{-4} M of

each cation. Integrated areas appear in parentheses. Columns utilized include a CS2 separator, CSC-2 suppressor and fiber-replacement column. Fiber bathed with 40.0 mM KIO_3 at 3.2 ml/min. Eluent, 7.0 mM HNO_3, pumped at 2.2 ml/min; injection volume, 20 μl; detector wavelength, 215 nm.

Figure 5. Representative chromatograms of IO_3^- at several injected concentrations by RIC (A) and dual-column IC (B). Columns utilized include AS3 separator, ASC-2 suppressor, and fiber-replacement column (latter column used only for RIC injections). Fiber bathed with 40.0 mM KIO_3 at 2.8 ml/min. Eluent, 10.0 mM NaOH, pumped at 2.0 ml/min; injection volume, 20 μl; detector wavelength, 215 nm.

Figure 6. Response produced by KIO_3, NaOH, NaCl, and HCl (each 10.0 mM) injected directly into the fiber-replacement column (IO_3^- form). Fiber bathed with 40.0 mM KIO_3 at 3.0 ml/min. Eluent, distilled water, pumped at 2.0 ml/min; injection volume, 20 μl; detector wavelength, 210 nm.

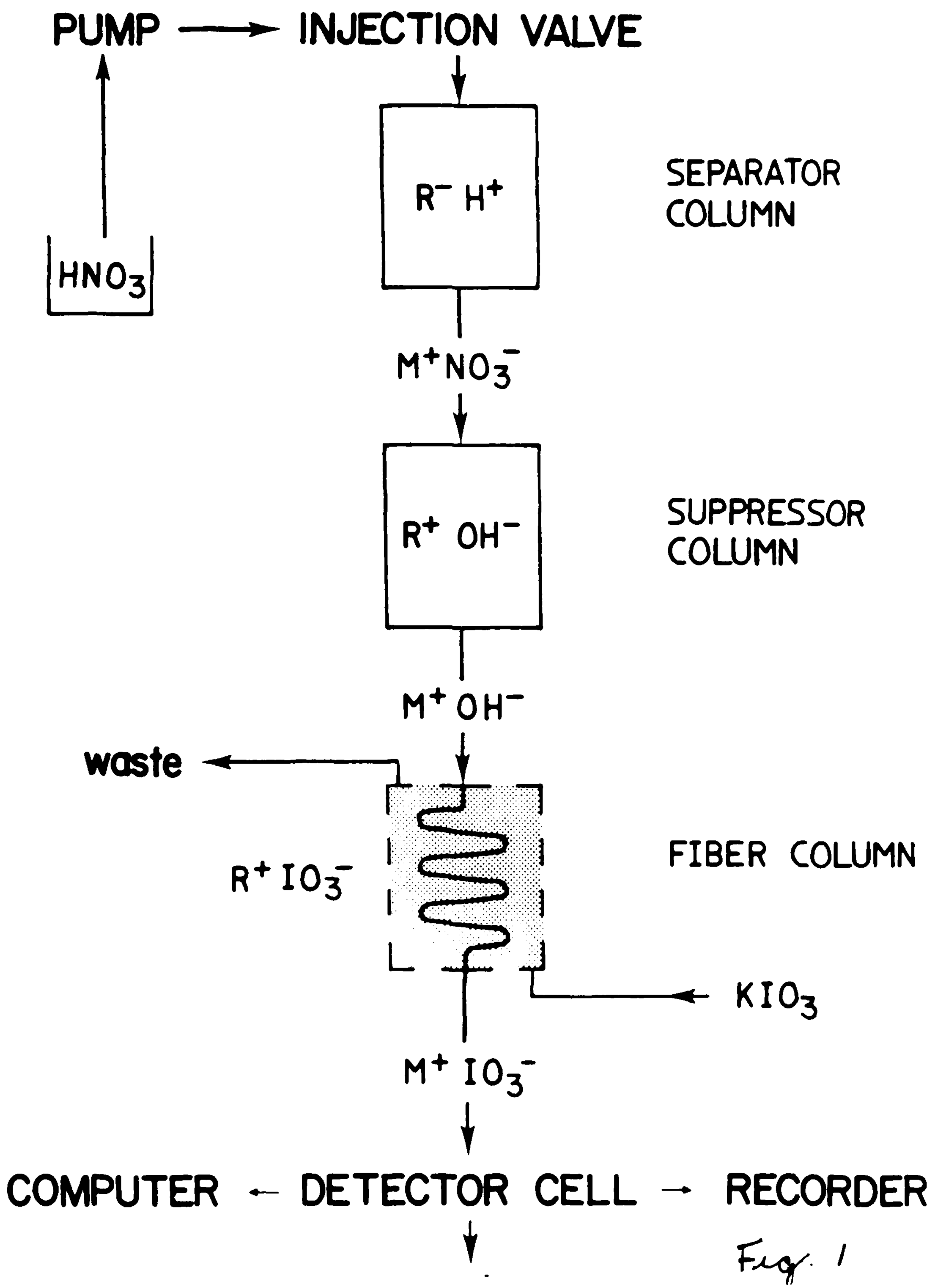
PUMP
INJECTION VALVE
HNO_3
$R^- H^+$
SEPARATOR COLUMN
$M^+NO_3^-$
$R^+ OH^-$
SUPPRESSOR COLUMN
$M^+ OH^-$
waste
$R^+ IO_3^-$
FIBER COLUMN
KIO_3
$M^+ IO_3^-$
COMPUTER
DETECTOR CELL
RECORDER

Fig. 1

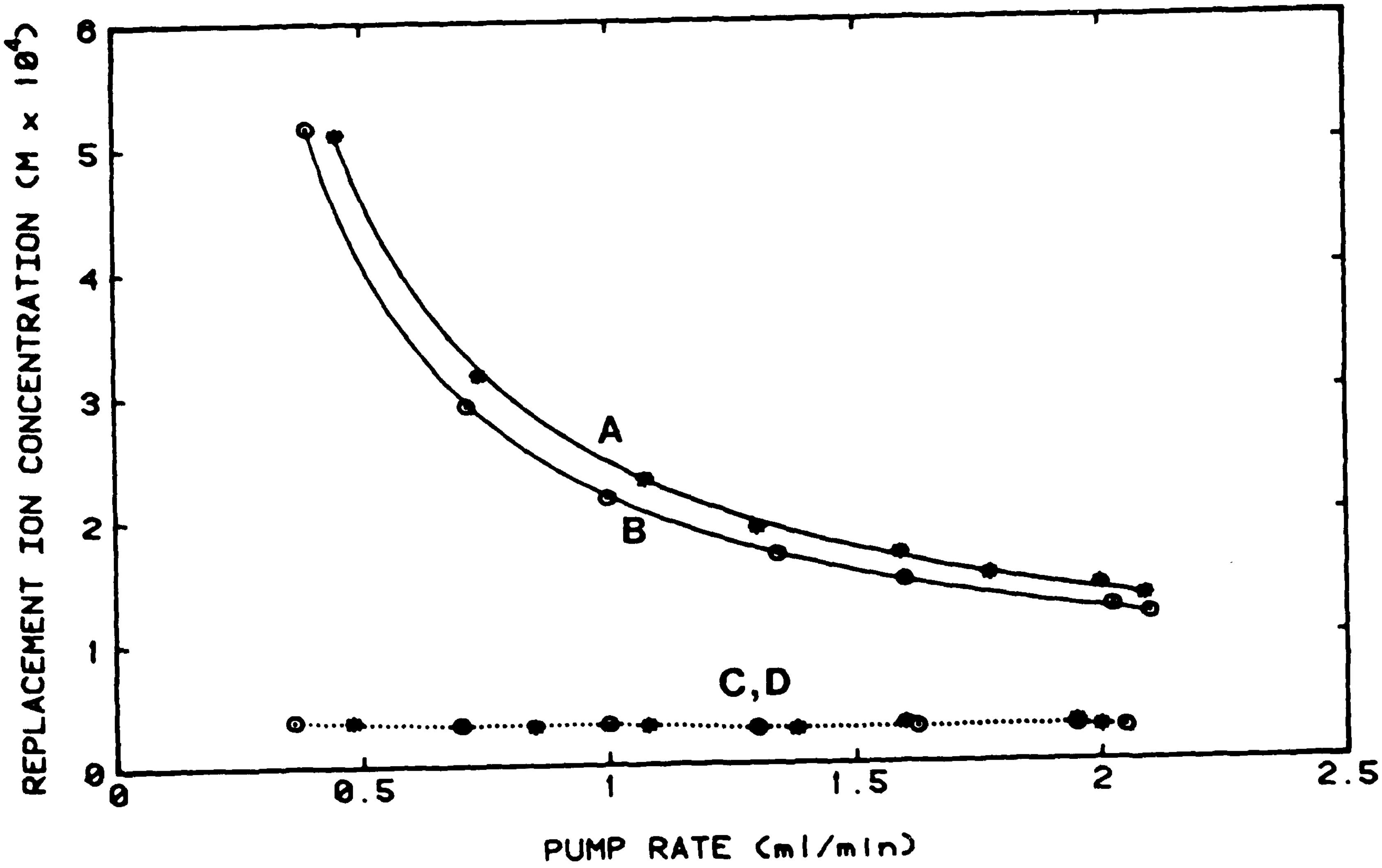
REPLACEMENT ION CONCENTRATION (M x 10⁴)
PUMP RATE (ml/min)
A
B
C,D
0
0.5
1
1.5
2
2.5
1
2
3
4
5
6

Fig. 2

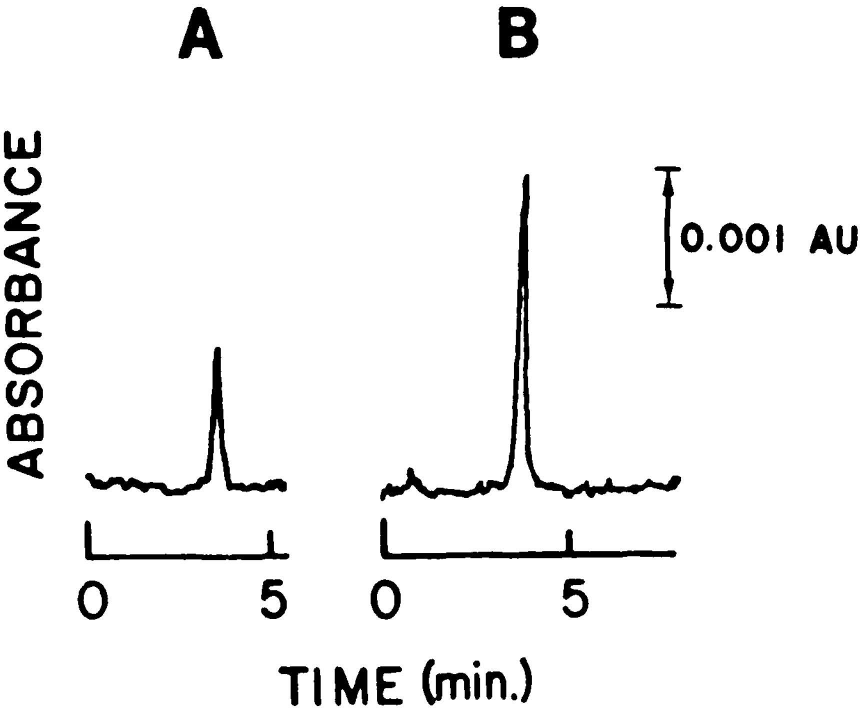

Fig. 3

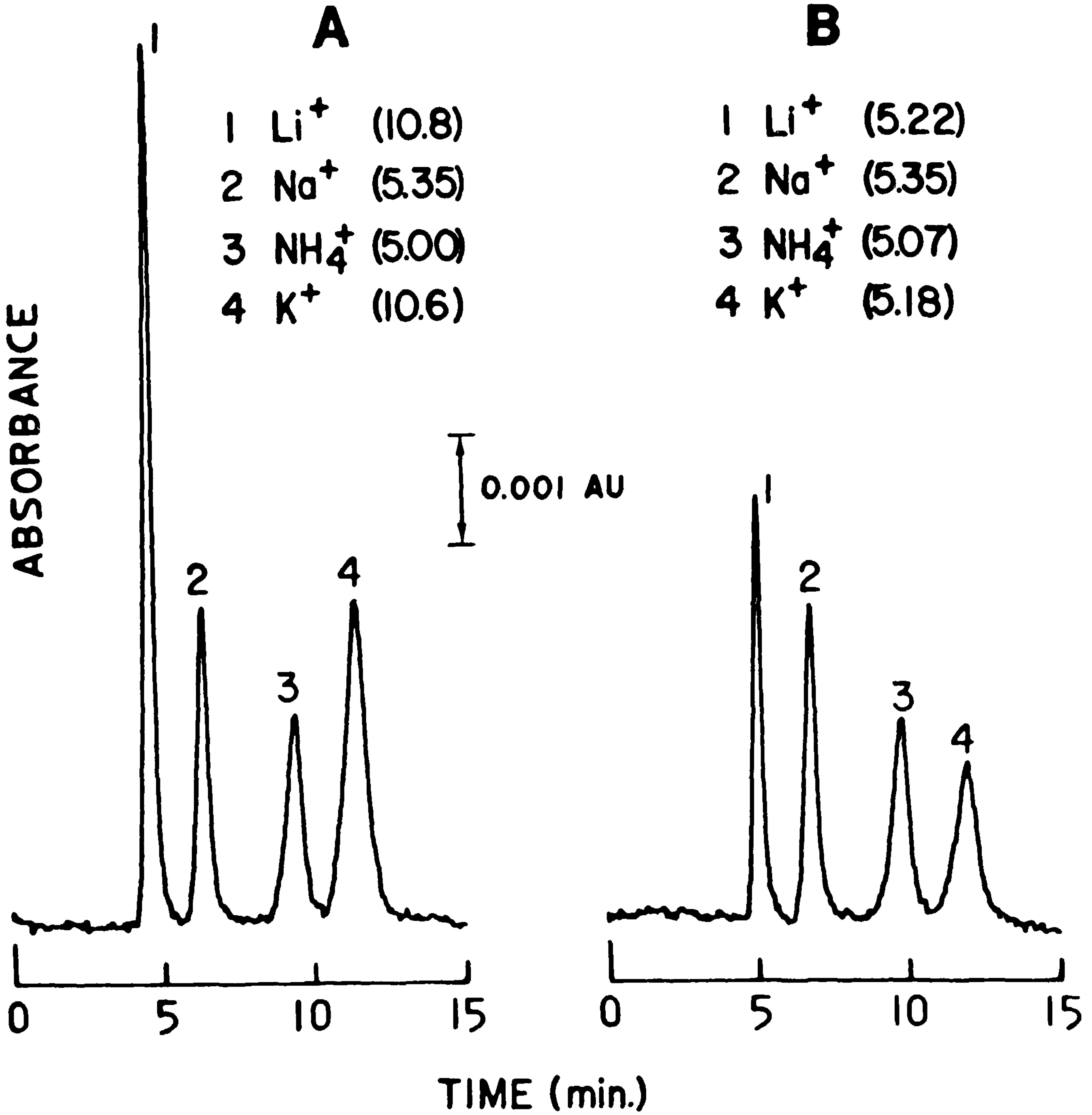

A
1 Li+ (10.8)
2 Na+ (5.35)
3 NH4+ (5.00)
4 K+ (10.6)
B
1 Li+ (5.22)
2 Na+ (5.35)
3 NH4+ (5.07)
4 K+ (5.18)
ABSORBANCE
0.001 AU
1
2
3
4
0
5
10
15
TIME (min.)

Fig. 4

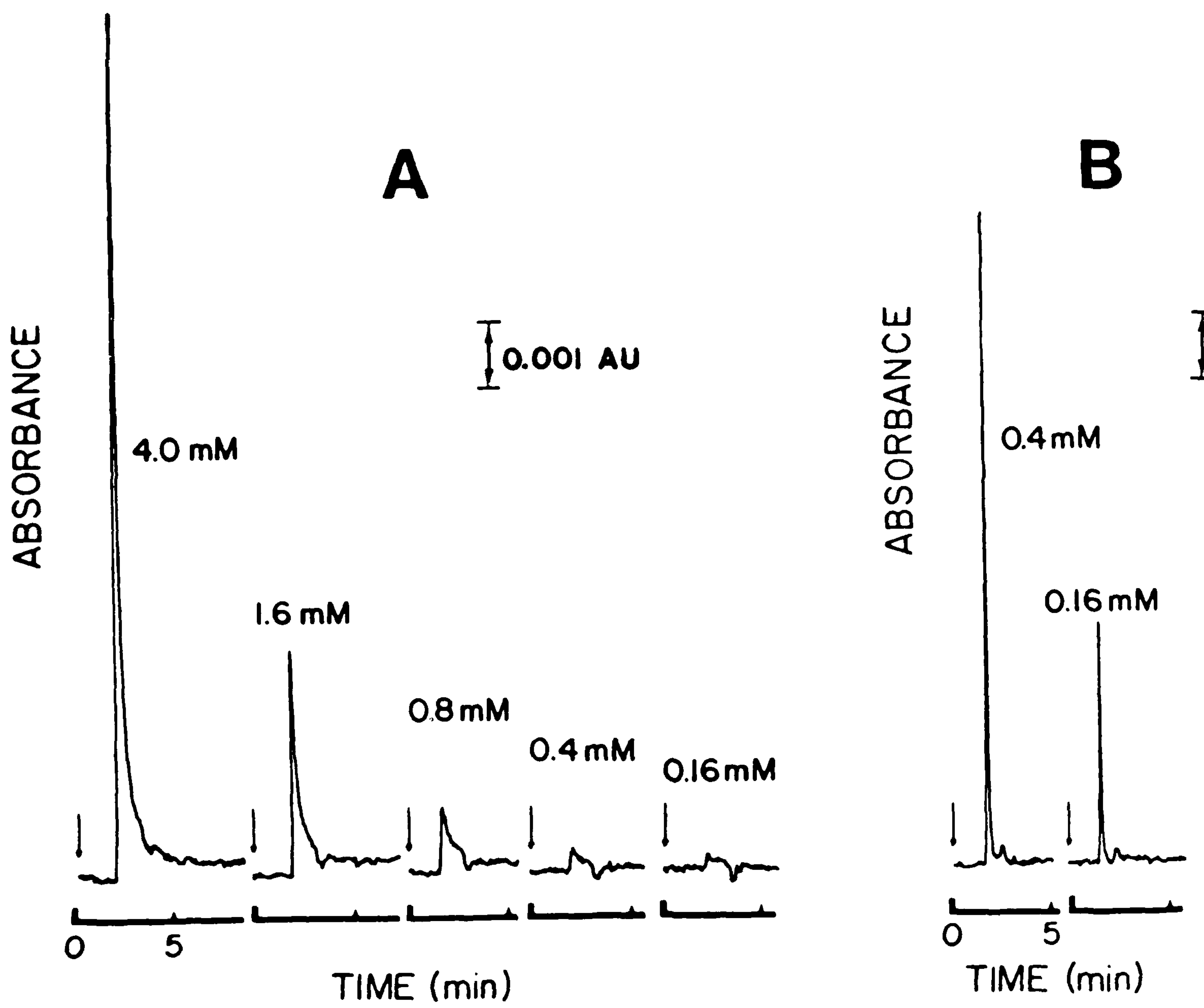
A
B
ABSORBANCE
0.001 AU
4.0 mM
1.6 mM
0.8 mM
0.4 mM
0.16 mM
0
5
TIME (min)
ABSORBANCE
0.001 AU
0.4 mM
0.16 mM
0
5
TIME (min)

Fig. 5

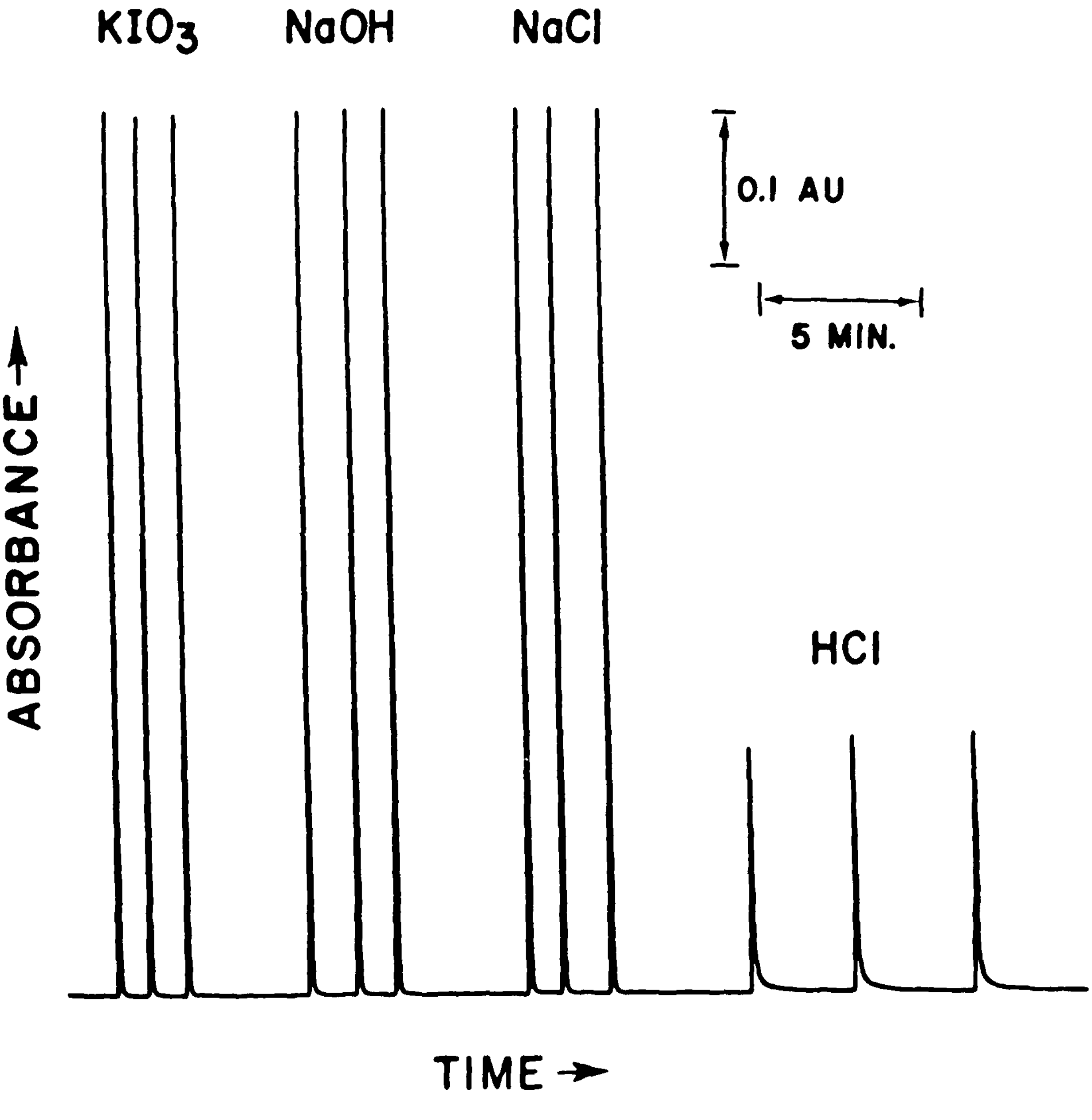

Fig. 6

TECHNICAL REPORT DISTRIBUTION LIST, GEN

	No. Copies
Office of Naval Research Attn: Code 1113 800 N. Quincy Street Arlington, Virginia 22217-5000	2
Dr. Bernard Douda Naval Weapons Support Center Code 50C Crane, Indiana 47522-5050	1
Naval Civil Engineering Laboratory Attn: Dr. R. W. Drisko, Code L52 Port Hueneme, California 93401	1
Defense Technical Information Center Building 5, Cameron Station Alexandria, Virginia 22314	12 high quality
DTNSRDC Attn: Dr. H. Singerman Applied Chemistry Division Annapolis, Maryland 21401	1
Dr. William Tolles Superintendent Chemistry Division, Code 6100 Naval Research Laboratory Washington, D.C. 20375-5000	1
Dr. David Young Code 334 NORDA NSTL, Mississippi 39529	1
Naval Weapons Center Attn: Dr. Ron Atkins Chemistry Division China Lake, California 93555	1
Scientific Advisor Commandant of the Marine Corps Code RD-1 Washington, D.C. 20380	1
U.S. Army Research Office Attn: CRD-AA-IP P.O. Box 12211 Research Triangle Park, NC 27709	1
Mr. John Boyle Materials Branch Naval Ship Engineering Center Philadelphia, Pennsylvania 19112	1
Naval Ocean Systems Center Attn: Dr. S. Yamamoto Marine Sciences Division San Diego, California 91232	1

END
DATE
FILMED
5-88
DTIC